Oceanologia, Vol. 66, No. 3, 2024
© Polish Academy of Sciences
Institute of Oceanology

https://doi.org/10.5697/ULWV7710

Mapping of morphological coastline changes based on aerial photographs and Discrete Fourier Transform, Hel Peninsula, Poland

Barbara Stachurska

Abstract

The coast is a dynamic zone where constantly occurring hydrodynamic and morphodynamic processes affect the shape of the shore. The paper presents a method based on spatial and spectral analysis of changes in the coastline position based on data obtained from aerial photographs interpretation and Fourier analysis, on the example of the Hel Peninsula. The Hel Peninsula is one of the most interesting accumulation forms of the Polish Baltic coast, where dynamic changes of the seashore cause the occurrence of time-varying sections of accumulation-abrasion of the coastline. For the purpose of detecting the coastline changes, historical aerial photographs from the years 1947, 1957, 1963, 1991 were used. It was assumed that the over-40-year research period, which includes the obtained series of aerial photographs, would allow for a sufficient study of the long-term shoreline changes, which allow for distinguishing the length of characteristic coastline undulations. The quasi-wave signal of the shoreline changes obtained from the aerial photographs interpretation, after using Fourier analysis, enabled an effective and precise identification of the coastline undulation. The spatial analyses, showed that the Hel Peninsula is clearly divided into a part subjected to accumulation processes and an abraded one. Furthermore, the dynamics of coastline changes was determined, showing that the abrasive processes were intensifying. Moreover, spectral Fourier analysis allowed for the precise identification of coastline undulations with dominant lengths. The obtained results of spatial and spectral analysis indicate that abrasive-accumulation sections with a length of about 0.3–4.5 km dominate on the Hel Peninsula shoreline.

Keywords

Aerial photography; Fourier analysis; Hel Peninsula; Coastline changes; Spatial analysis; Spectral analysis

Institute of Hydro-Engineering, Polish Academy of Sciences, Kościerska 7, 80–328 Gdańsk, Poland
Correspondence: b.stachurska@ibwpan.gda.pl
Received: 18 November 2022; **revised:** 22 April 2024; **accepted**: 22 May 2024

1. Introduction

The analysis of the variability and erosion-accumulation trends of coastlines is the basis for a wide range of research undertaken by coastal scientists and engineers. Although strictly defined for practical purposes as the line of intersection of water and land surface, the dynamic nature of this border and its dependence on the temporal and spatial scale requires the use of a number of additional shore analysis indicators. Coastal areas that change over time are dynamic in nature, therefore, the term coastline used by coastal researchers is as dynamic as the feature it defines. Coastline identification is divided into two stages: firstly, it requires the selection and definition of a coastline feature indicator (i.e. base of cliff, dune base line, high-water line etc.), and secondly, it involves the detection of the selected coastline feature from the available data sources (i.e. the research methodology) (Boak and Turner, 2005). Mapping the shoreline using various techniques for obtaining data and capturing its characteristics makes it easier to locate and understand the trend of changes in the shoreline. Measurable predictions of the future evolution of the coastline in erosion-affected areas are essential for effective coastal zone planning and management (Appeaning Addo et al., 2008). They allow for the timely capture of threats to sandy beaches around the world, responsible for damage and destruction of coastal infrastructure (Ferreira et al., 2006).

Numerous data sources are available for studying coastline positions. However, in the majority of coastal areas, historical data are often limited, non-existent, or vary in scale and regional extent. Consequently, the selection of data for use in a particular area largely depends on data availability (Boak and Turner, 2005). Methods for identifying shoreline positions vary. These include historical aerial photographs, which provide general information such as the presence of specific morphological features, but often lack details such as scale or reference objects (Dolan et al., 1983). Historical coastal maps, despite potential errors in scale, reference changes, and distortions due to storage conditions and the passage of time (Anders and Byrnes, 1991; Shoshany and Degani, 1992; Moore, 2000), offer valuable historical data not available from other sources. Beach surveys and GPS shoreline mapping with modern equipment offer higher precision but are limited to specific locations (Overton and Fisher, 1996). Remote sensing and multispectral methods cover larger areas but are hindered by pixel resolution limitations and associated costs (Cracknell, 1999). The use of a geographic information system and remote sensing technology allows for quantitative analysis of changes in the topography as well as the morphology of coastal areas (Yang et al., 2010). The most common shoreline detection technique used for visible shoreline features is manual visual interpretation, based on aerial photography (List and Farris, 1999). Visual photointerpretation may include shoreline extractions made from aerial photographs, and numerous studies using this technique indicate its high effectiveness (Dolan et al., 1978; Collier et al., 2001; Dellepiane et al., 2004; Liu and Jezek, 2004; Constantino et al., 2020). The data obtained from the shoreline extraction can be presented in the form of a discrete signal, as a harmonic curve, thanks to which the methods of filtering in the frequency domain can be used for the analysis (Gehrmann and Harding, 2018), which include algorithms based on the Fourier transform. Rayner (1972) was among the first to use the Discrete Fourier Transform (DFT) method for spatial classification and regionalization based on terrain patterns described formally by harmonic components. Ricard et al. (1987) employed spectral analysis to study the topography of the Basin and Range Province, while Idier and Falques (2014) analyzed shoreline undulations along the Atlantic coast of Africa using the DFT method. The methods based on Fourier analyses (i.e., DFT) (Dudgeon and Mersereau, 1983) deserve special attention because their application can detect which components are present in the signal and in what relative 'amounts' they appear.

The Hel Peninsula is one of the most interesting accumulation forms of the Polish Baltic coast. The undulation of the Hel Peninsula coastline depends on many factors such as surrounding hydrodynamic conditions, its geological structure, or human impact. It is an area where dynamic changes related to the interaction of the lithosphere and the hydrosphere of the seashore occur. The constantly occurring hydrodynamic processes due to waves, sea currents, and morphodynamic processes related to accumulation and abrasion affect the shore morphology. The Hel Peninsula exhibits a dual nature, both in terms of its deep geological structure and its development during the Holocene Period. Its formation began after the Atlantic transgression, when the sea level stabilized 1–2 meters below today's level (Tomczak, 1995). The Peninsula reached its current shape around 1000 years ago, when the sea level rose by about 1.5 meters, resulting in the flooding of coastal areas (Tomczak, 1995). The Peninsula's geological structure, along with prevailing hydrodynamic conditions, has led to the development of erosion-accumulation forms along its shoreline. The sea shores of the Hel Peninsula, which are exposed to abrasion processes, are being destroyed at an alarming rate, and this concerns, to varying degrees, the individual sections of the peninsula. The open seashore is characterized by both accumulative as well as abraded sections (Zawadzka-Kahlau, 1999; Stachurska, 2012).

This article focuses on presenting a method for analyzing aerial photographs aimed at identifying changes in coastline position, using the Hel Peninsula as an example. Four series of aerial photographs from the years 1947–1991 were used, from which orthophotomaps were made. The results obtained from spatial analysis, representing a quasi-wave signal of the shoreline position, were subjected to spectral Fourier analysis. The primary objective of the present paper is to present a method that determine the long-term shoreline changes in over a 40-year research period. Moreover, the identification of the developmental directions of the Hel Peninsula shoreline, and the classification of its segments subjected to abrasion processes as well as those undergoing accumulation, were also undertaken. In addition, qualitative and quantitative analyses of changes in the position of the coastline were carried out to determine the dynamics of its development. Obtained results give possibility to determine the regions which are most exposed to abrasion processes and those in which the accumulation dominates as well as to extract large-scale spatial changes of the shoreline. Moreover, the method of aerial photograph analysis used, present an opportunity to perform spectral analysis, using Fourier transform, owing to which the most dominant lengths of shoreline undulations were determined. Spectral Fourier transformation is presented here as a specialized technique for coastline analysis, not previously used in the area of the Hel Peninsula. The results obtained demonstrate that the tools employed in this study complement each other, enabling the acquisition of reliable and detailed descriptions of changes in coastline position.

2. Regional setting

Due to its unique natural and landscape features, the Hel Peninsula is an extremely valuable part of the Polish coast. The Hel Peninsula is located in the north of Poland and separates the Bay of Puck from the Baltic Sea. The length of the peninsula from the port in Władysławowo to the headland, measured along the shore of the open sea, is slightly less than 35 km. In the narrowest point, between Chałupy and Kuźnica, the width of the peninsula amounts to about 150 m, increasing towards the headland and near the town of Hel, where it reaches a width of 3000 m.

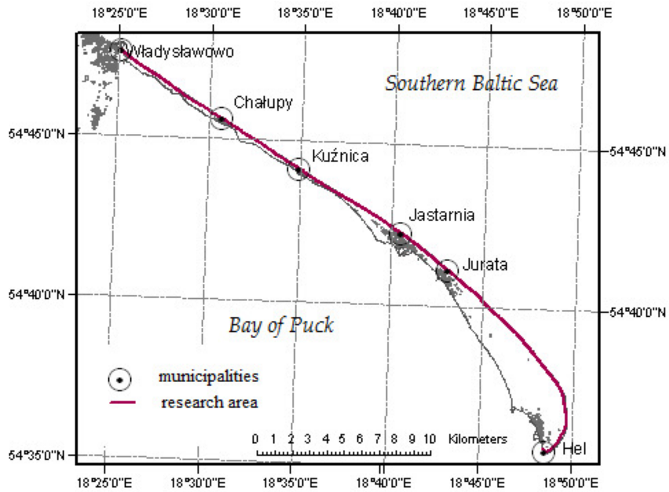

Figure 1. Location of the research area.

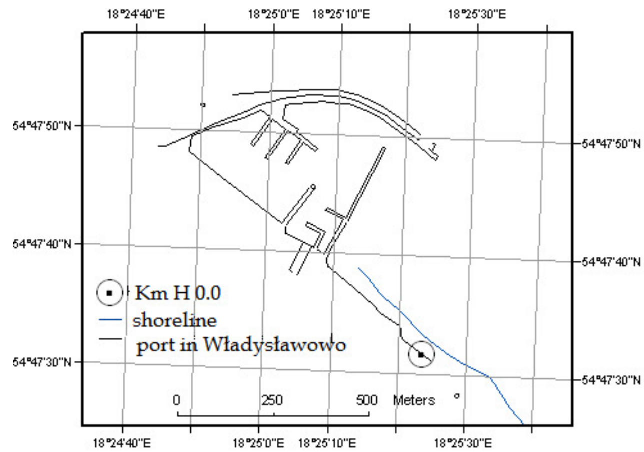

Figure 2. Location of the starting point of the Hel Peninsula (km H 0.0) in relation to the breakwater in the port of Władysławowo.

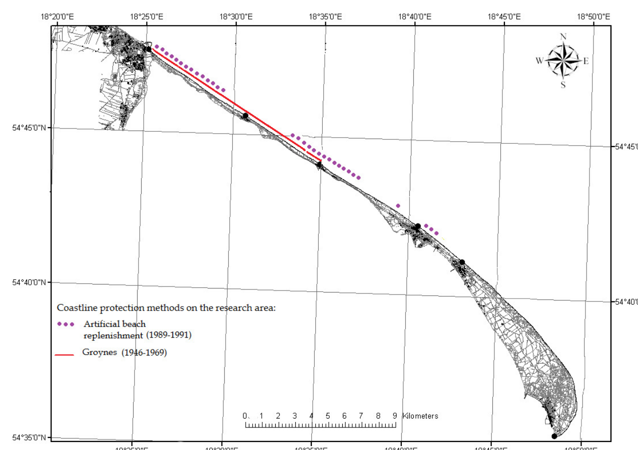

Figure 3. The schematic sketch illustrates the localization of coastal protection methods employed between 1947 and 1991 on the open sea side of the Hel Peninsula coast.

The territorial scope of this work covers the coastal zone of the Hel Peninsula on the open sea side, from the port in Władysławowo to the port in Hel (Figure 1).

The starting point (km H 0.0) was the place defining the base of the Peninsula at the local shoreline kilometer mark. This point was identified on the shoreline of the open sea, approximately 350 m east of the eastern breakwater of the port in Władysławowo (Figure 2).

The coastal zone of the Hel Peninsula is constantly impacted by dynamic processes, including waves, currents, and sea level fluctuations. Long-term hydrodynamic and meteorological factors play a significant role in shaping changes along the coastline. The atmospheric circulation in the South Baltic basin is characterized by prevailing westerly winds, specifically from the southwest, west, and northwest directions, which drive sediment transport along the eastern shore of the Hel Peninsula. During storms, short and steep waves of considerable height form, primarily driving the transformation of the coastline. When analyzing the dynamic factors influencing the development of the Hel Peninsula coastline, attention should also be given to rip currents, which can affect the shallow water zone, particularly in areas with coastal protection structures such as groynes, where alternating accumulation and abrasion forms are observed.

Anthropogenic influences are significant factors shaping the coast of the Hel Peninsula, primarily associated with the adverse effects of human activities such as urbanization, tourism, recreation, and industrialization. Urbanization in coastal areas often disrupts natural dune ecosystems, necessitating efforts to strengthen the coastline, which, in turn, disturbs natural shoreline processes. During the analyzed period in the studied area of the Hel Peninsula, two systems of groynes built between 1946 and 1969 were present (the red line in Figure 3). A group of wooden groynes (114 pieces) was located at km H 0.02–10.19, while 48 reinforced concrete groynes were constructed at km H 10.25–12.32 (Basiński et al., 1993). Severe storms in the 1980s prompted the implementation of artificial beach replenishment measures in certain sections of the Hel Peninsula coast (see violet dots in Figure 3). The primary sections subjected to artificial beach replenishment until 1991 were km H 0.0–4.5 and km H 9.5–13.6 (Dubrawski, 2000).

3. Boundary definitions

The shape of dune coasts varies. Among the various forms of relief, certain permanent elements can be distinguished that occur along the entire dune coast. These include the beach, located in front of the dune, which stretches directly along the water surface, ranging from a dozen to

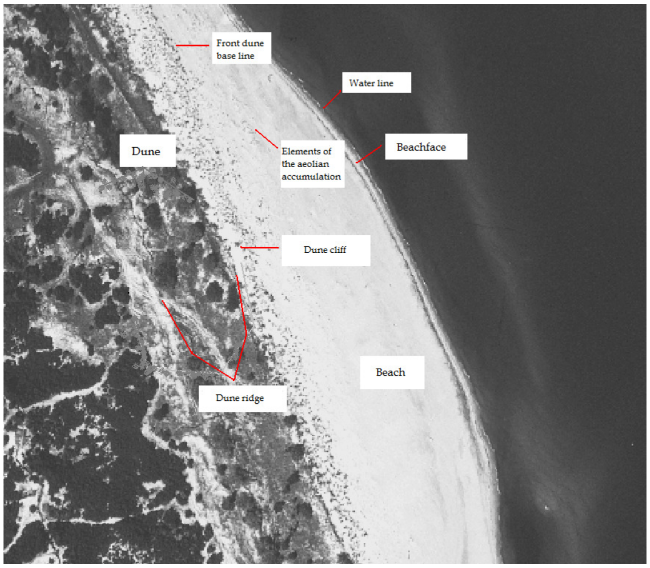

Figure 4. Morphological elements of the dune coast.

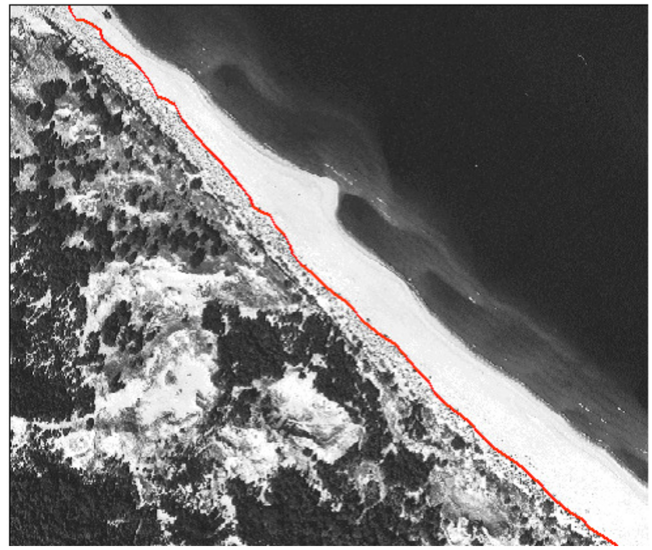

Figure 5. An example of the front dune base line marked on the aerial photo from 1991. Area between Jurata and Hel (km H 25).

over a hundred meters wide. Typically, the beach is completely devoid of vegetation but may feature elements of aeolian accumulation landforms. Behind the beach lies an artificially formed embankment known as the front dune, mostly planted with grass (Królikowski and Strzelecki, 1969). Beyond the front dune, there are areas of the so-called dune ridge, which stretch parallel to the shoreline. The morphological elements of the dune coast visible in the aerial photograph are presented in Figure 4.

The definition of a coastline is very broadly understood. It depends on the type of shore, the way of looking at the coastal zone, the type of information that is intended to be obtained from the analysis of this area, and the type and size of cartographic materials used. The shore is primarily a zone of interaction between the marine and land environments. Thus, the shore has a time-varying width and so, the precise determination of the boundaries of this zone is difficult due to the gradual changes in the environment (Urbański, 2001). The contact point of both environments, sea and land, is usually presented on large-scale maps in a linear manner (Larson et al., 2003). Several coastlines, i.e., lines that can be distinguished on the shore, can be marked on aerial photos. These lines are, for example, the line of intersection of the land surface with the sea surface, commonly called the water line, the front dune base line, or dune crest line. In practice, in order to determine the areas of abrasion and accumulation based on aerial or satellite images, the position of the water line or the position of the front dune base line is analyzed. Determining the position of the dune base line is relatively simple, while the precise location of the water line is extremely difficult to establish. It should be remembered that even on the basis of tacheometric measurements performed on the beach, it is possible to determine only an instantaneous position of the water line, which, due to sea level fluctuations and waves, does not have to reflect the morphodynamic processes occurring in the studied area. Therefore, it is commonly believed (Shoshany and Degani, 1992; Furmańczyk and Musielak, 1993; Kaczmarek et al., 1998) that the best way to determine accumulation / abrasion areas based on aerial or satellite images is to analyze changes in the position of the front dune base line. Qualitatively and quantitatively, it reflects the interaction of aero- and hydrodynamic factors occurring on the shore and allows the identification of development trends (Furmańczyk and Musielak, 1993; Zawadzka-Kahlau, 1999). Therefore, in a later stage of this work, it was decided to carry out analyses of the position changes on the basis of the front dune base line. In the case of the Hel Peninsula, the front dune embankment is mainly planted with sand grass (*Ammophila arenaria* L.), and the optically visible boundary between the beach (sand) and the seaward edge of the dune vegetation was used to interpret aerial photographs as a front dune baseline (Figure 5).

4. Material and methods

The aerial photographs were obtained from the Military Geographical Institute in Warsaw, Poland. Four series of archival aerial photos of the Hel Peninsula were used for the analysis. They were taken in 1947, 1957, 1963, and 1991 on a scale of 1:10 000. A total of 105 black and white aerial photographs were used in this study: 32 photos from 1947, 33 from 1957, 17 from 1963, and 23 photos from 1991. For the purposes of this work, the negatives of the photos have been scanned. The schematic arrangement of all aerial photographs, already linked to a coordinate sys-

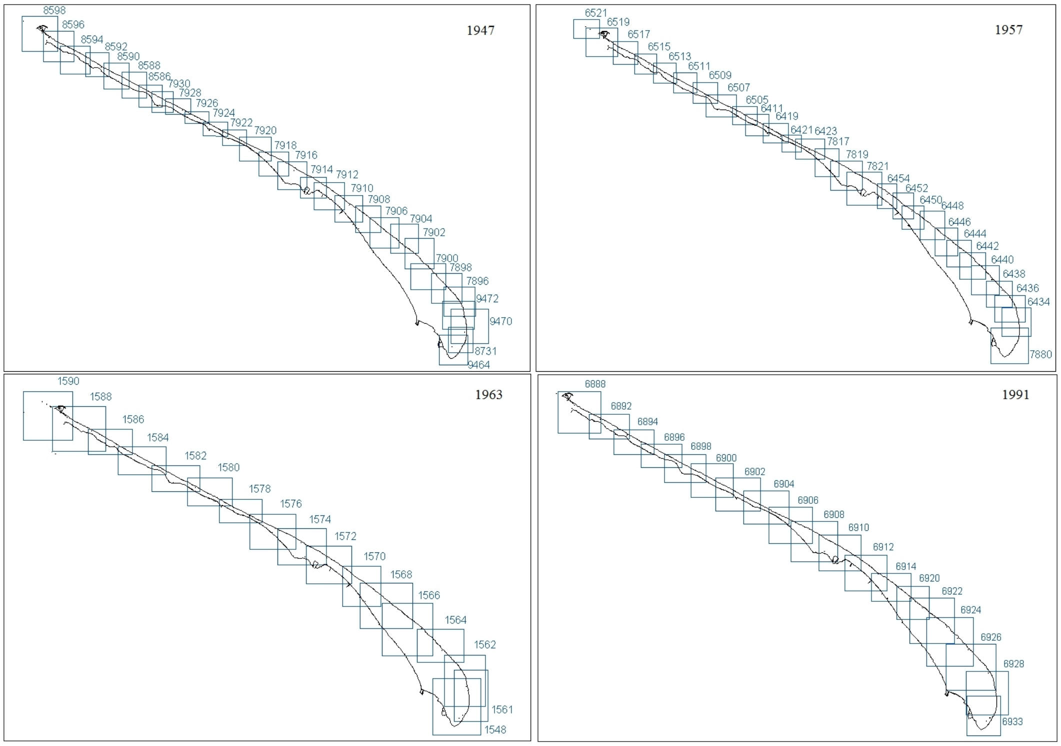

Figure 6. Arrangement diagram of aerial images scans for years 1947, 1957, 1963, 1991.

Table 1. The details of all aerial photographs used in the present research.

Date	Scale	Number of photos	Photo number
1947	1:10 000	32	8598, 8596, 8594, 8592, 8590, 8588, 8586, 7928, 7926, 7924, 7922, 7920, 7918, 7916, 7914, 7912, 7910, 7908, 7906, 7904, 7902, 7900, 7898, 7896, 9472, 9470, 8731, 9464
1957	1:10 000	33	6519, 6517, 6515, 6513, 6511, 6509, 6507, 6505, 6411, 6419, 6421, 6423, 7817, 7819, 7821, 6454, 6452, 6450, 6448, 6446, 6444, 6442, 6440, 6438, 6436, 6434, 7880
1963	1:10 000	17	1590, 1588, 1586, 1584, 1582, 1580, 1578, 1576, 1574, 1572, 1570, 1568, 1566, 1564, 1562, 1561, 1548
1991	1:10 000	23	6888, 6890, 6892, 6894, 6896, 6898, 6900, 6902, 6904, 6906, 6908, 6910, 6912, 6914, 6920, 6922, 6924, 6926, 6928, 6933

tem, is shown in Figure 6. In the Table 1 the execution date, scale and number of all aerial photos used is presented.

4.1 Aerial photograph processing

Aerial photos obtained from scans have a raster format. The first stage of their processing was the georeferencing process to display them in a given coordinate system without changing their content. Reference points with constant geographic coordinates were selected. In this case, a railway track (Figure 7) and a building located on the headland of Hel Peninsula (Figure 8) were used. Next, rectification was carried out, whereby the raster cells of the photos were converted into new ones, aligned with the coordinate system. This process requires resampling, i.e., calculating new values for the raster cells. In this work, resampling of the analyzed aerial photos was carried out using the nearest neighbor method, assigning the value of the nearest pixel. The geographic coordinate system WGS_1984_UTM_Zone_34N was used. The georeferencing process relying on a numerical topographic map of the Hel Peninsula on a scale of 1:10 000 was carried out. All analyses were performed in the ArcMap program.

In the vector technique, the basis of the image is a point with specific coordinates. Digitization is the main element of vector analysis. Joining several points creates a curve or a polygon. The layers created as a result of this process were saved as .shp files. Files of this format can contain three types of objects; points, lines, and polygons, and their values can be edited in attribute tables. In order to carry out the present analyses, the digitization process was carried out using the front dune base line and the railway track line, which was the reference point for these analyses, and at the same time, a permanent element in the aerial photographs of all series. The basic element of a

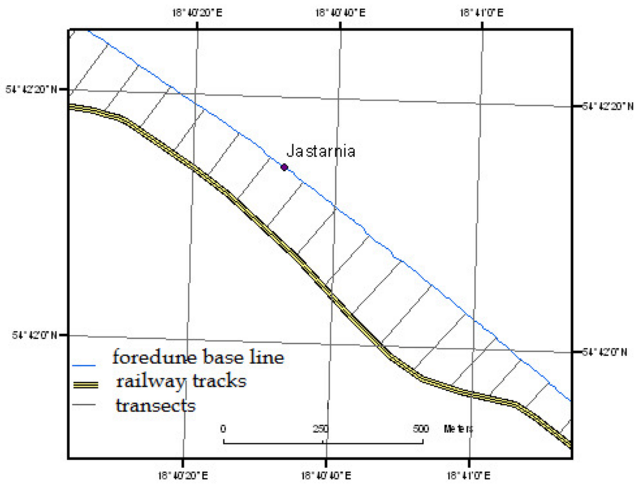

Figure 7. The arrangement of the perpendicular transects between the railway tracks and the foredune base line in Jastarnia.

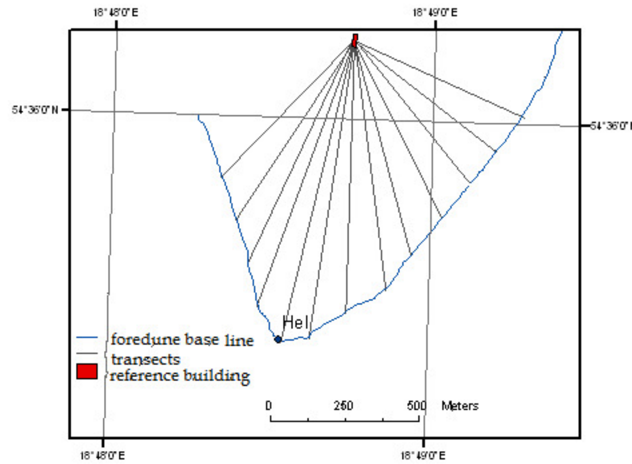

Figure 8. The arrangement of the radial transects between the reference building and foredune base line on the headland of the Hel Peninsula.

Table 2. Types of spatial analysis operations used.

Spatial analysis operations	Description
Rasterization	The process of transforming vector data into a raster form consisting of assigning an "id" identifier of a given object to the raster cell.
Reclassification	Assigning a new map of classes to cells according to the established new key.
Map algebra	Multiplication, subtraction, addition, and division of layers.
Allocation	NoData values are assigned to the values of the nearest cells.
Vectorization	The process of data transformation from raster to vector form.

Table 3. Front dune base line shift classes [m].

Classes	1947–1957	1957–1963	1963–1991	1947–1991
1	$-60 \div -40$	–	$-60 \div -40$	$-100 \div -75$
2	$-40 \div -30$	$-40 \div -30$	$-40 \div -30$	$-75 \div -50$
3	$-30 \div -20$	$-30 \div -20$	$-30 \div -20$	$-50 \div -25$
4	$-20 \div -10$	$-20 \div -10$	$-20 \div -10$	$-25 \div 0$
5	$-10 \div 0$	$-10 \div 0$	$-10 \div 0$	$0 \div 25$
6	$0 \div 10$	$0 \div 10$	$0 \div 10$	$25 \div 50$
7	$10 \div 20$	$10 \div 20$	$10 \div 20$	$50 \div 75$
8	$20 \div 40$	$20 \div 40$	$20 \div 40$	$75 \div 100$
9	$40 \div 60$	$40 \div 60$	$40 \div 60$	$100 \div 125$
10	–	> 60	–	–

Table 4. Front dune base line rate of changes classes [m year^{-1}].

Classes	1947–1957	1957–1963	1963–1991	1947–1991
1	–	$-7 \div -5$	–	$-2 \div -1$
2	$-5 \div -3$	$-5 \div -3$	–	$-1 \div 0$
3	$-3 \div -1$	$-3 \div -1$	$-3 \div 1$	$0 \div 1$
4	$-1 \div 0$	$-1 \div 0$	$-1 \div 0$	$1 \div 2$
5	$0 \div 1$	$0 \div 1$	$0 \div 1$	$2 \div 3$
6	$1 \div 3$	$1 \div 3$	$1 \div 3$	–
7	$3 \div 5$	$3 \div 5$	$3 \div 5$	–
8	$5 \div 7$	$5 \div 7$	–	–
9	–	> 7	–	–

raster map is a pixel (raster). The position of a raster cell is determined by its coordinates in the adopted reference frame. Raster map cells can contain integer numbers used to define qualitative data and real numbers that define quantitative data (Urbański, 2001). In this work, five types of spatial analysis operations were carried out, presented in the appropriate order in Table 2.

The results of analyses carried out on aerial photographs of the offshore side of the Hel Peninsula were divided into two parts. First, the changes in the position of the front dune base line were determined, then the rates of changes in the front dune base lines were calculated.

In order to determine the changes in the front dune base line position, reference objects were selected (railway tracks and buildings) as permanent elements in the aerial photographs of all series. Then, starting from km H 0.0, the transects extending between the railway track line and the front dune base line (Figure 7) were determined at intervals of approximately 100 m. These profiles were oriented perpendicularly to the front dune base line. In addition, radial profiles were marked from the building located in the center of the Hel headland to the front dune base line (Figure 8).

The transects between the railway tracks and the front dune base line from earlier years were subtracted from the length of the sections from later years. The resulting shift amounts of the front dune base line position were divided into classes (Table 3). The same classification classes were used for the periods 1947–1957, 1957–1963, and 1963–1991. The period 1947–1991 was treated in a separate way due to its length and, hence, the averaged measurement values.

Vector and raster analyses of the rate of changes to the front dune base line were carried out analogously to the method of calculating the changes in the position of the dune base line. Four series of aerial photographs were divided into four computational periods. The dune base line rate of change was calculated in [m year^{-1}] and is presented in Table 4.

5. Analysis and interpretation of the results

5.1 Assessment of cartometric measurement errors

Despite the great usefulness of aerial photographs, it is important to note that errors often occur during the collection and digitization of photographs (Cohen et al., 1996; Tuominen and Pekkarinen, 2004). Measurement errors in aerial photos can occur at various stages of the work being carried out. Errors can be classified as either geometric or radiometric in origin, and either systematic or random in form (Morgan et al., 2010). Geometric errors may occur due to problems with the equipment used to capture the photographs or flying and shutter speeds (Paine and Kiser, 2012). The analysis of the relationship between the resolution of the camera and the ground resolution for multiple scales of aerial photography carried out by Morgan et al. (2010) showed that for aerial photos on a scale of about 1:10 000, the highest error was 1.22 m. Similar values were presented by Jensen (2000), who determined a resolution error of approximately 5 m for photographs at a scale of 1:40 000 and an error of around 2.5 m for photos at a scale of 1:20 000. The assessment of the accuracy of measurements from aerial photographs also indicated the importance of considering the so-called graphic error of the map, which refers to errors in determining the location of the coastline. Therefore, for photos at a scale of 1:10 000, the average error value (m_d) of the coastline measurement can be calculated using the formula (Pelczar et al., 1990):

$$m_d = s \times 0.357\,\text{mm} \tag{1}$$

where s is the map scale denominator.

Therefore, in the case of the 1:10 000 aerial photography scale, in order to calculate changes in the coastline position, an graphic error of $+/-3.5$ m should be taken into account. This error magnitude is analogous to the findings of Zawadzka-Kahlau (1999), who estimated the graphic error for maps at a scale of 1:25 000 to be approximately $+/-9$ m.

Thus, it was assumed that in the present method, the

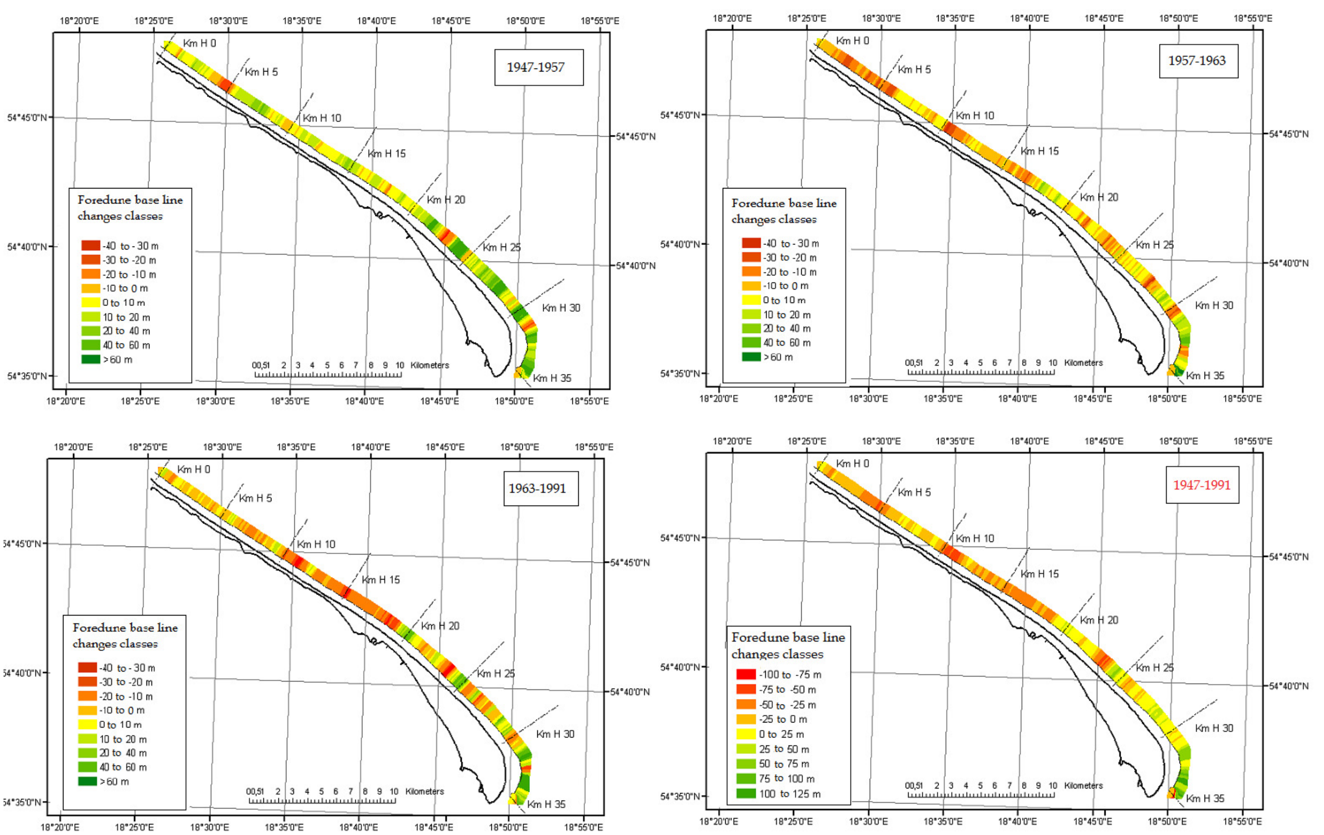

Figure 9. Coastline shift maps depicting changes in the position of the front dune base line for the time periods: 1947–1957, 1957–1963, 1963–1991, and for 1947–1991.

Table 5. Abrasive-accumulative changes in the foredune base line of the offshore side of the Hel Peninsula.

Period	Abrasion [km]	Abrasion [%]	Acumulation [km]	Acumulation [%]	Balance [km]	Balance [%]
1947–1957	17.0	49.7	17.2	50.2	0.2	0.5
1957–1963	20.4	59.6	13.8	40.4	−6.6	−19.2
1963–1991	22.0	64.3	12.2	35.7	−9.8	−28.6
1947–1991	20.2	59.06	14.0	40.9	−6.2	−18.6

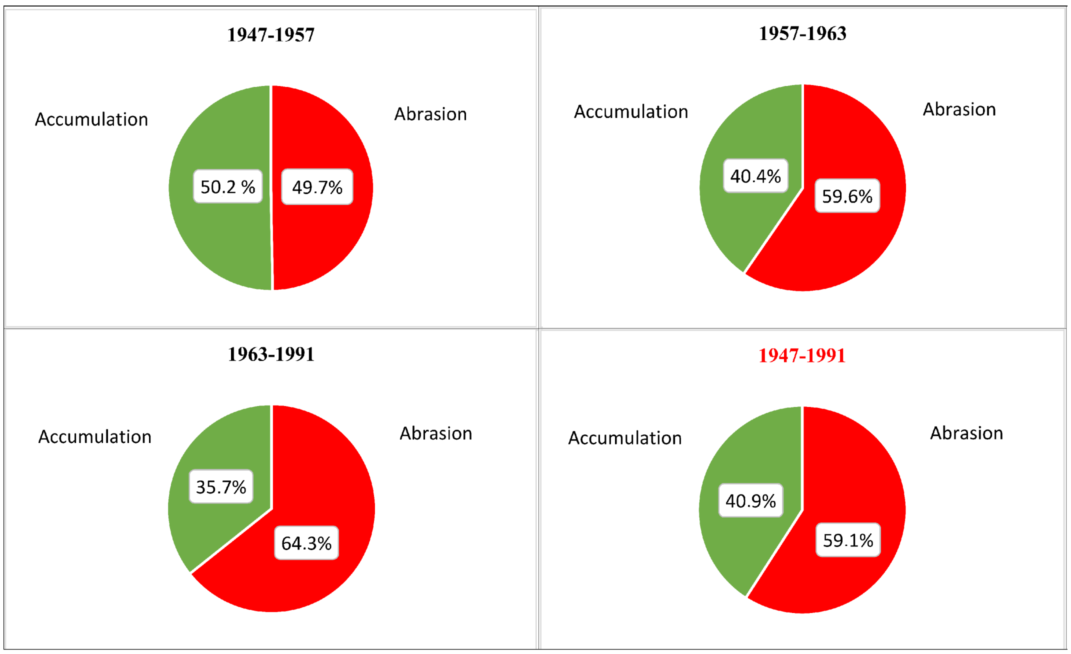

Figure 10. The balance of changes in the position of the front dune base line for all analyzed time periods.

total error obtained by summing up the two measurement errors (the resolution of aerial photography and the accuracy of measurement) was of the order of +/−5 m.

Highly accurate reference data are crucial because the spatial accuracy of the corrected product depends on the geometric quality of the reference layer (Hughes et al., 2006; Morgan et al., 2010). Therefore, in the present research, two key processes were employed during aerial photograph processing: georeferencing and rectification. These processes aim to prevent geometric displacement errors and provide spatial reference.

5.2 Quantitative changes in the coastline shape. Coastline shift maps

Analysis of the aerial photographs allows the obtaining of quantitative changes in the position of the coastline. The results of the front dune base line changes are presented for the periods 1947–1957, 1957–1963, 1963–1991, and 1947–1991 (The shift map of the position of the front dune in the period 1947–1957 shows three main abrasive areas: section km H 4.5 ÷ 5.0, km H 23.0 ÷ 24.0, and km H 31.0 ÷ 32.0. The abrasion values in the above-mentioned sections ranged from 35 m to 45 m. Additionally, eight accumulation areas per km H 7.0 ÷ 8.0, 14.0 ÷ 15.0, 22.0, 24.0, 28.0, 30.0, 32.0, and on km H 33.0 are shown. Accumulation values in these areas ranged from 22 m to 60 m. A relatively stable area was found in section 8 ÷ 20 km H. In section 20 ÷ 35 km H, the processes of accumulation of the front dune base line prevailed. Finally, it was established that in the period 1947–1957, a total of 17 km of the front dune were abraded, and 17.2 km accumulated (Table 5). Between 1947 and 1957, 49.7% of the research area experienced abrasion (Figure 10).

Analysis of the differential line for the period 1957–1963 (Figure 9) shows that the areas of accumulation of the front dune base line were recorded at km H 18 ÷ 19, km H 29, km H 31 ÷ 32.5, and km H 33 ÷ 34. Accumulation values in the above-mentioned areas ranged from 25 meters to approx. 60 m (km H 33 ÷ 34). Strongly abraded regions were found at km H 0 ÷ 6, km H 10 ÷ 12, km H 22, km H 28, km H 30 as well as km H 32. The abrasion values in the above-mentioned locations ranged from 17 to 43 meters. The results indicate that a total of 20.4 km of the front dune base line was abraded in the period 1957–1963, whereas only 13.8 km of the front dune was accumulated (Table 5). During the period 1957–1963, 59.6% of the research area experienced abrasion (Figure 10).

The coastline shift map for the period 1963–1991 (Figure 9) showed a predominance of abrasive processes, especially in the central and western areas of the Hel Peninsula. The central part of the peninsula, from km H 10.0 to 19.0, was almost completely covered by abrasion processes. Abrasion values ranged from 20 meters to approx. 50 m. Areas with a predominance of accumulation processes were found in four regions of the Peninsula: at km H 20 ÷ 21, 24 ÷ 25, 31, and 32 ÷ 34. Accumulation values ranged from 35 meters at km H 24–25, to 100 meters at km H 33 ÷ 34. The front dune base line shift map for the period 1963–1991 showed a uniformly abraded area in the central part of the Hel Peninsula in the section km H 10 ÷ 19. On the eastern and western sides of the abraded region, abrasive-accumulation systems were observed, with the eastern side characterized by a predominance of accumulation processes, and the western side – by abrasive ones. In the period 1963–1991, a total of 22 km of the front dune were abraded, and 12.2 km were accumulated (Table 5). Between 1963 and 1991, 64.3% of the research area experienced abrasion (Figure 10).

The analysis of the position of the differential line of the over-40-year-long research period 1947–1991 (Figure 9) shows that the Hel Peninsula displayed the duality of abrasive-accumulation processes. It was found that sections at km H 0.0 ÷ 20.0 and 23.0 ÷ 24.0 were covered by abrasion processes, while the eastern part of the peninsula, at km H 25.0 ÷ 34.0, was dominated by accumulation processes. In the period 1947–1991, abrasion covered 20.2 km of the peninsula front dune, while accumulation covered only 14 km (Table 5).

The balance of changes in the position of the front dune base line, presented in Figure 10 and Table 5 indicates a decisive prevalence of abrasive processes in the years 1957–1963, 1963–1991, and 1947–1991. Only in the period 1947–1957 did the accumulation process prevail, albeit insignificantly. Overall, abrasive changes showed an increasing tendency and the dynamics of the front dune destruction processes intensified over time. In the research period 1957–1963, the balance of changes showed a prevalence of abrasion over a stretch of 6.6 km, while in the period 1963–1991, it was already 9.8 km. The time-averaged results of the analyses for the period 1947–1991 also show the dominance of destructive processes. The abrasion covered 6.2 km more of the front dune base line than the accumulation. This situation is influenced by several factors, including hydrodynamic conditions, the geological characteristics of the Peninsula, and human activities such as coastal protection measures, which disrupt the coastal system. Additionally, sea levels along the southern coast of the Baltic Sea are rising. Mareographic data from Gdańsk shows that the sea level increased from 4.6 mm per year during the period of 1886–1906 to 5.7 mm per year between 1970 and 1990 (Uścinowicz et al., 2014).

5.3 Qualitative changes in the coastline shape. Dynamics of coastline changes

The pace of shifting of the front dune base line well-characterizes the direction and dynamics of the shore development. It reflects the real development of the accumulation and abrasion process (Zawadzka-Kahlau, 1999) as a qualitative tool of the system dynamics (Khairulbahri, 2022). The qualitative changes refer to the shift that occurs when the shoreline system moves from one state – accumulation, to erosion, and determines the dynamics of this phenomenon. The results of analyses are graphs showing the change rates of the position of the front dune base line for the periods 1947–1957, 1957–1963, and 1963–1991 and the map of the front dune base line change rates for the multi-year period of 1947–1991 is presented in Figure 11.

In the ten-year research period 1947–1957 (Figure 11), the highest accumulation velocity of the front dune base line is about 6 m year^{-1} and was recorded for km H 33.0. The area with the fastest abrasion rate was noted for km H 5.0, where the front dune base line retreated by about 4 m year^{-1}.

The research period 1957–1963 (Figure 11) was characterized by very strong abrasive changes along practically the entire analyzed shore of the Hel Peninsula. The highest front dune abrasion rates, of about 7 m year^{-1}, were recorded at km H 28.0, while the highest rates of dune increment, of about 7 ÷ 9 m year^{-1}, were recorded at km H 33.0 ÷ 34.0.

In the period 1963–1991 (Figure 11), the abrasive and accumulative change rates of the front dune base line that occurred were slight along the section from km H 0.0 ÷ 10.0. The highest accumulation velocity, equal to about 4 m year^{-1}, was seen at km H 33.0. The fastest loss of the front dune occurred at km H 11.0, 19.0, 24.0, and 32.0, where the foredune base line was retreating at a rate of about 2 m year^{-1}.

The analysis of the front dune base line change rates in the over-40-year period 1947–1991 (Figure 11) shows averaged-in-time abrasive-accumulation systems on the offshore side of the Hel Peninsula. The significant sections of the shoreline, at km H 0.5 ÷ 4.0, 5.0 ÷ 6.5, and 12.0 ÷ 18.0, where the front dune was retreating at a rate of more than 1 m year^{-1} have been identified. The sections at km H 4.0 ÷ 5.0, 10.0 ÷ 12.0, and 35.0 were characterized by an abrasion rate of approx. 2.0 m year^{-1}. Regions with an accumulation rate of the front dune base line of over 0.5 m year^{-1} were recorded for the sections at km H 20 ÷ 21, 26, 29, 30. A higher rate of the accumulative process was found at km H 25, 32, and 33 ÷ 34, where the front dune accumulation rate varied from 1.5 m year^{-1} for H 25 and

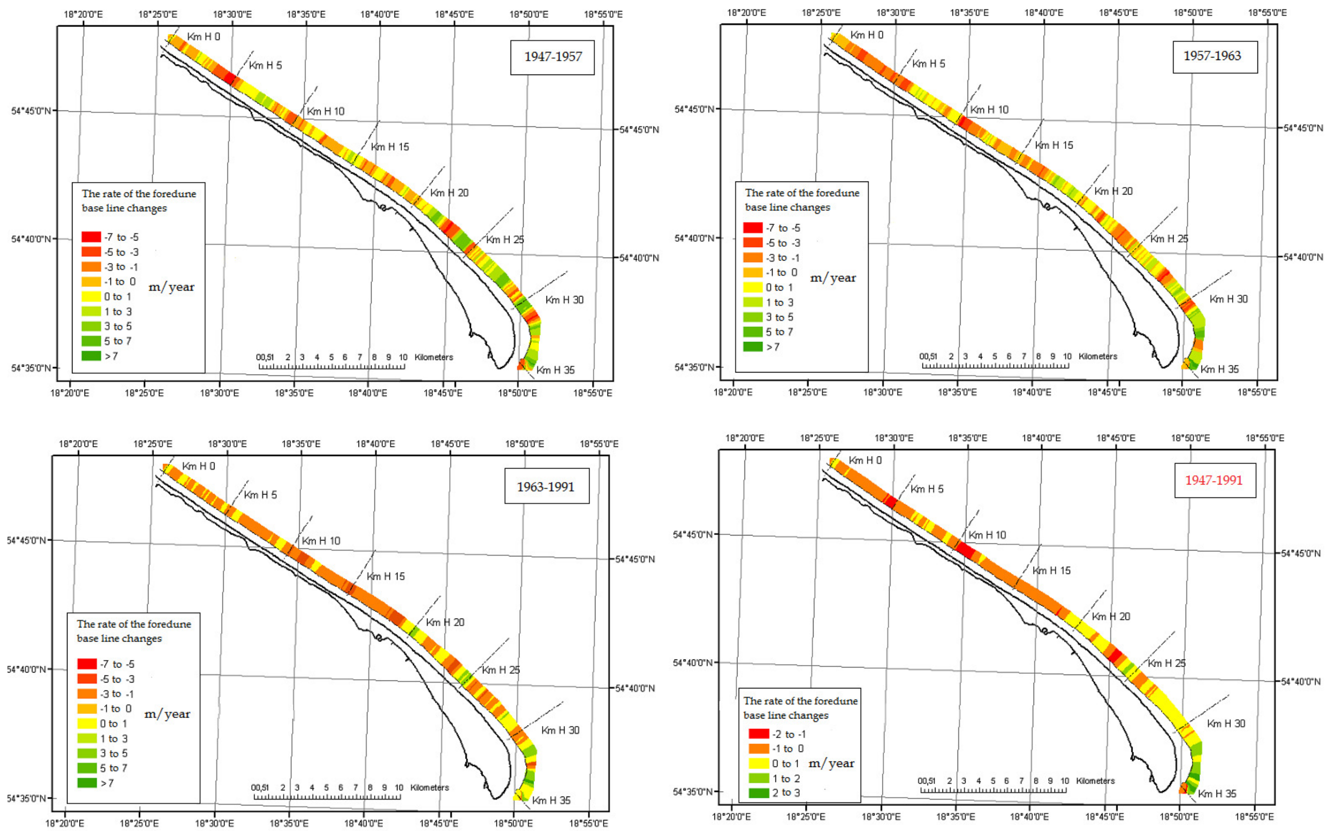

Figure 11. Maps of change rates of the front dune base line, for time periods: 1947–1957, 1957–1963; 1963–1991 and for 1947–1991.

32 km, to 2.5 m year^{-1} for H 33 ÷ 34 km.

Based on the presented graphs of the foredune base line change rates (Figure 11), sections with a constant accumulative tendency and regions with a predominance of abrasion were identified. It was found that the most highly-eroded sections in all the analyzed periods were located at km H 4.0 ÷ 6.0, 11.0, and 35.0, while the area with the highest accumulation values was recorded at km H 33.0. Areas with a significantly different development direction were observed at km H 18.0 ÷ 19.0, 22.0, 28.0, 30.0, and 32.0.

As anticipated, a comparative analysis of the coastline shift maps and the change rates in the position of the front dune base line for all investigated periods allowed the conclusion that the maximum velocity of the front dune retreat was identified in the sections where predominantly abrasive processes dominated. On the other hand, the most intense accumulation process was correlated with the highest rate of front dune restoration.

It was found that the dynamics of changes in the position of the front dune were definitely higher in the eastern part of the Hel Peninsula. The periods 1947–1957 and 1957–1963 were characterized by a particularly high rate of change. The analysis of changes in the shores of the offshore side of the Hel Peninsula showed greater intensity of erosion in the western and central parts. Particularly endangered stretches of beach were at km H 0.0 ÷ 7.0, 10.0 ÷ 18.0, and 23.0 ÷ 34.0 in the areas of Chałupy, Kuźnica, and Jurata. It was found that the abrasive processes in the western and central parts of the Hel Peninsula were intensifying. The part of the Hel Peninsula from 10 ÷ 24 km H was particularly endangered.

6. Discussion

6.1 Spatial analysis

The analysis of changes in the position of the offshore foredune base line of the Hel Peninsula allowed identifying alternately located abrasive and accumulative sections. The distribution of these segments was of a quasi-wave nature. Treating the shoreline position changes as a quasi-wave signal, spatial analysis was performed by determining the locations where the amplitude of the change was close to 0 as well as the points where the shoreline position deviated significantly from the equilibrium position, thereby distinguishing the so-called nodes (stable places) and antinodes (places of significant shore shifts). The theory of wave-pattern development of the shore was presented by Furmańczyk (1994). He found that on the Hel Peninsula shore, the distances between successive nodes occur most

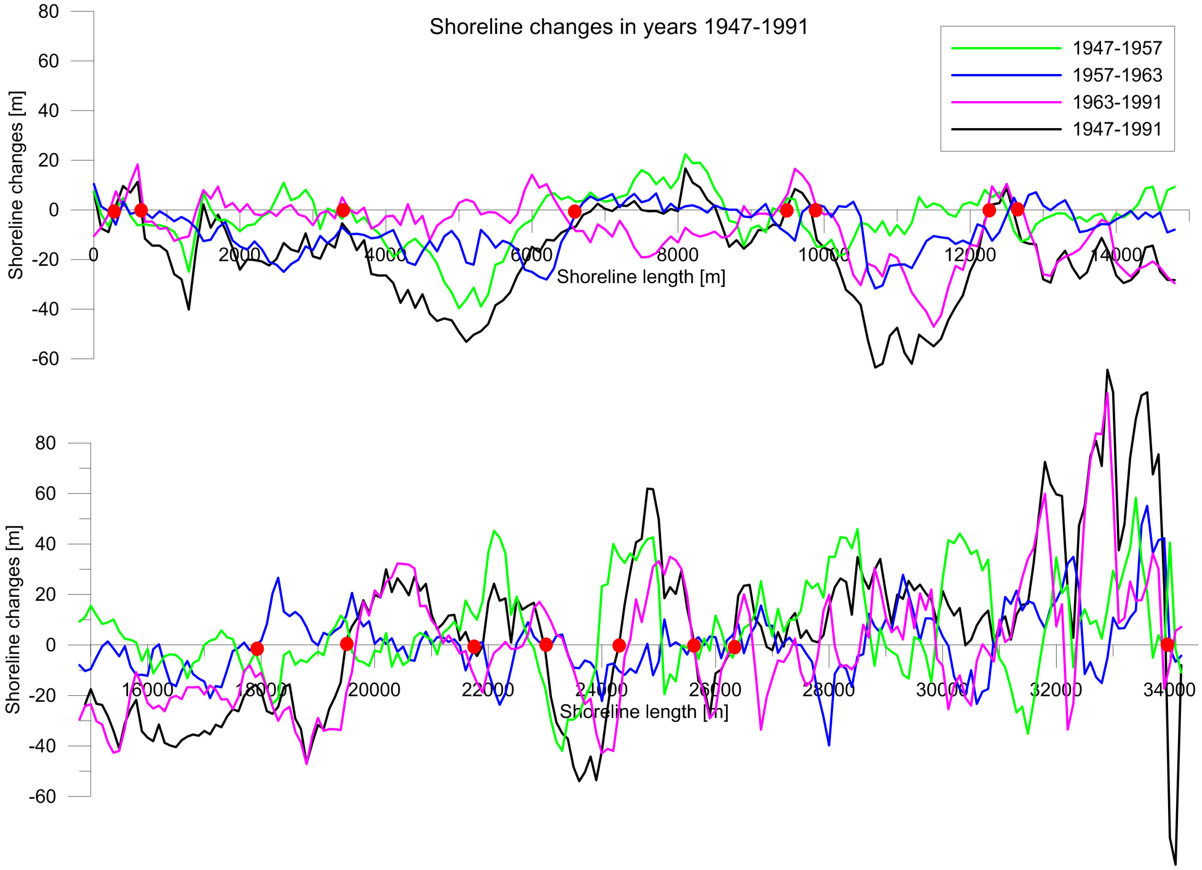

Figure 12. Shoreline position changes in the period 1947–1991. Nodes are marked by red dots.

frequently in two distance ranges; 1 ÷ 3 km (mezo generation) and 3 ÷ 5 km (macro generation).

The analysis of the results from the years 1947, 1957, 1963, and 1991 (Figure 12) allowed the detection of nodal points located at km H 0.3, 0.5, 3.5, 6.5, 9.5, 10.0, 12.2, 12.5, 18.0, 19.5, 21.8, 23.0, 24.2, 25.5, 26.3, and 34.0.

Analysis of the aerial photography data allowed 16 nodal points to be identified (Figure 12). These points indicate where the coastline changed the least and made it possible to determine the sections corresponding to antinodes, i.e., the areas where the amplitudes of the shoreline deviation are characterized by significant shore shifts (accumulation-abrasive sections). Five accumulation-abrasive sections with a length shorter than 1.0 km were found, four with a length longer than 1 km but shorter than 2 km, four with a length of about ∼3.0 km, and additionally, one with a length of 5.5 km, and one with a length of 7.7 km. This means that, according to Furmańczyk's theory, five detected accumulation-abrasive sections were shorter than the mezo generation (<1 km), eight sections belong to the mezo generation (1 ÷ 3 km), and only two sections of antinodes conditionally belong to the macro generation (3 ÷ 5 km). The obtained results can be compared with the results of Zawadzka-Kahlau (1999), which showed the minimum and maximum lengths of the abrasive-accumulation sections to be 0.5 and 12 km, respectively. In the present work, the maximum length of the accumulation-abrasive section was found to be 7.7 km, and the minimum length was 0.5 km. After Zawadzka-Kahlau (1999), the abrasive-accumulation sections of the Hel Peninsula were divided into three classes with different length ranges. Class I ranged from 4 km and more, class II included sections with lengths from 2 to 3.5 km, and class III included sections with lengths from 0.5 to 1.5 km. As a result of this division, in the period 1947–1991, two sections with lengths of 5.5 km and 7.7 km were distinguished, belonging to class I. Six abrasive-accumulation sections belonging to class II were identified, and seven sections belonging to class III with lengths of 0.5, 0.7, 0.8 km, 1.5 km, 1.2 km, 1.2 km, and 1.3 km were determined. Table 6 presents

Table 6. The number of abrasion-accumulation sections for the period 1947–1991 according to the classes proposed by Furmańczyk (1994) and Zawadzka-Kahlau (1999).

Furmańczyk (1994)	< 1.0 km 5	1.0–3.0 km 8	3.0–5.0 km 2
Zawadzka-Kahlau (1999)	0.5–1.5 km 7	2.0–3.5 km 6	> 4.0 km 2

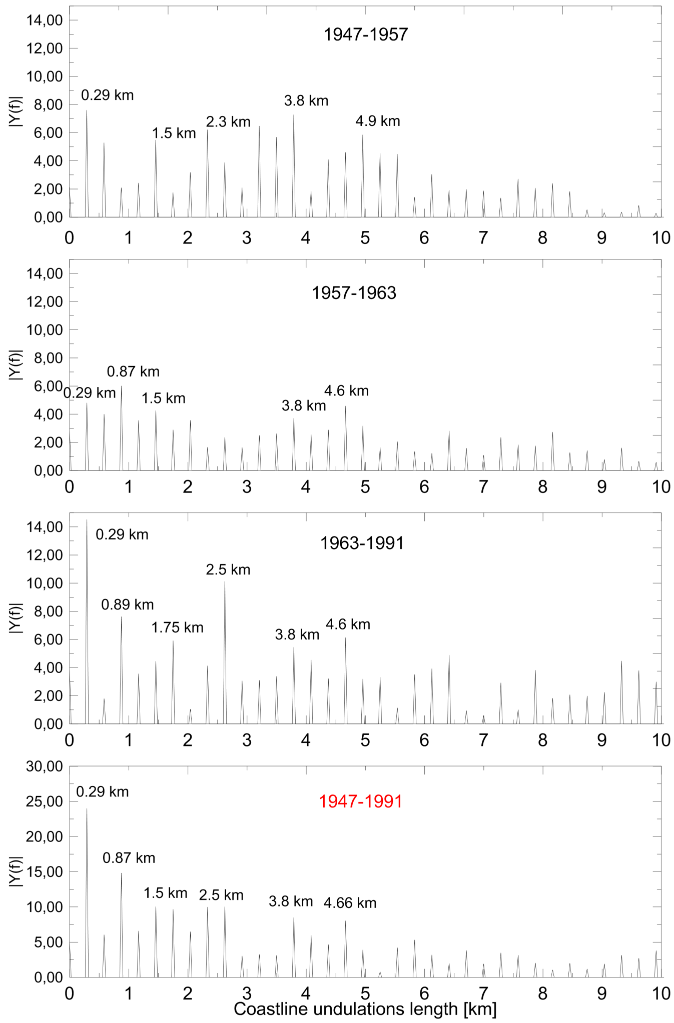

Figure 13. The Hel Peninsula shoreline undulation lengths for periods (a) 1947–1957, (b) 1957–1963, (c) 1963–1991, and (d) 1947–1991 resulting from DFT analysis.

the lengths of abrasion-accumulation sections proposed by Furmańczyk (1994) and Zawadzka-Kahlau (1999), as well as the number of sections of specific lengths resulting from spatial analysis based on aerial photographs of the research presented.

The obtained results of spatial analyses indicate that the abrasive-accumulation sections with a length of 0.5–3.5 km are dominant along the seashore line of the Hel Peninsula.

6.2 Spectral analysis

The quasi-signal of the front dune base line position changes was analyzed by applying the Discrete Fourier Transform (DFT) method, which allowed for the conversion of the signal from the space domain into the frequency (wavelength) domain, thus enabling the identification of coastline undulations with dominant lengths. This method was chosen to provide sufficiently accurate results (Prošek and Leskovar, 2015). DFT analysis has been successfully used in many works aimed at determining the morphology, bathymetry, or topology of studied areas (Rayner, 1972; Idier and Falques, 2014; Spagnolo et al., 2017; Davis and Chojnacki, 2017; Gehrmann and Harding, 2018).

DFT was used in the present work to analyze the trends in the variability of the coastline position. The method consists of finding the characteristic scales on which the evolution of the coastline takes place in the space domain. Fourier series represent a periodic signal as an infinite sum of harmonic components that repeats its pattern over some period (Cooley and Tukey, 1965). Spectral analysis of the coastline assumes that the waves of the shoreline profiles are composed of sine waves of different wavelengths and amplitudes. The frequencies which have maximum peaks are the most important frequencies affecting the shape of the coastline signal. Fourier analysis makes it possible to determine the frequencies of the components included in a data series and enables a signal to be mapped from the space domain to the frequency domain (Gehrmann and Harding, 2018).

A MATLAB script was developed to process the data for the shoreline position changes by the Fourier transform. As a result of the analysis, a frequency plot, called a periodogram (Figure 13), was obtained. The Fourier analysis enables the determination of the lengths of the dominant accumulation-abrasive sections.

The Discrete Fourier Transform analysis was carried out with the spatial increment of 100 m (a distance between pairs of neighboring transects) for every 34 km H investigated. Therefore, the analysis allows for the identification of the shoreline undulations with minimum lengths that are approximately equal to twice the spatial step (i.e. 200 m). Ideally, the signal used in the Fourier analysis should have the same amplitude value at the first and the last discrete spatial points. However, for the real data obtained from measurements, such a situation is rare. Therefore, a signal filter was used to squeeze the tested signal to zero, in order to avoid so-called spectral leakage, which could obscure the appropriate frequencies. Likewise, function zero-padding was used to make the size of the input sequence equal to a power of two.

Figure 13 shows the distribution of the quasi-signal of the shoreline changes into its frequency components, which are represented here by the coastline undulation lengths [km]. The statistically significant periodicities of morphological coastline changes range from 0.29 to 3.8 km. The results in Figure 13 show precisely that the most dominant coastline undulation length occurred at the fundamental frequency equal to 0.29 km for almost all analyzed periods. The second harmonic is pronounced at 0.87 and the subsequent at 2.5, and 3.8 km.

The obtained results are consistent with the spatial analysis results. Spectral analysis allowed the location of the exact lengths of the accumulation-abrasive sections and established that they most often occur in the length range of 0.3 to 4.5 km.

7. Conclusions

The analysis of aerial photographs from the years 1947–1991 enabled the determination of coastal changes along the open sea shores of the Hel Peninsula. This analysis facilitated the identification of development trends in this area and the classification of abrasive and accumulation sections of the coast. It was observed that the Hel Peninsula comprises abraded western and central areas and an accumulated eastern area, with changes in the position of the front dune baseline exhibiting a quasi-wave pattern.

Qualitative analysis of the rate of coastline shift allowed for the determination of the dynamics and direction of coastline development. The results indicate that the eastern part of the Hel Peninsula experiences more intensive erosion compared to the western part, while the abrasion process in the western and central areas is escalating.

Based on the interpretation of aerial photoparaphs and the classification of abrasion-accumulation section lengths on the Hel Peninsula according to Furmańczyk (1994) and Zawadzka-Kahlau (1999), it was determined that coastal undulations of 0.5–3.5 km dominate the studied area of the Hel Peninsula.

Moreover, the quasi-wave signal of the Hel Peninsula shoreline changes, analyzed through Discrete Fourier Transform (DFT), facilitated the effective and precise identification of dominant coastline undulation sections ranging from approximately 0.3 to 4.5 km.

The aerial photo interpretation method has been proven to be an effective tool in shoreline research, enabling both qualitative and quantitative assessments of development trends in the studied area. Additionally, Fourier analysis of shoreline undulation signals provided precise information about the dominant lengths of abrasion-accumulation sections.

In summary, the combination of tools used in this study complement each other, resulting in reliable and detailed descriptions of coastline position changes.

Acknowledgment

The results presented in this study were obtained as part of the Polish State Committee for Scientific Research project No. 3P04E05624 Assessment of the sediment balance in the process of abrasion of the Hel Peninsula shore carried out from 2003–2006 at the Faculty of Oceanography of the University of Gdańsk and as part of the statutory activities of the Institute of Hydro-Engineering of the Polish Academy of Sciences in Gdańsk.

References

Anders, F., Byrnes, M., 1991. *Accuracy of shoreline change rates as determined from maps and aerial photographs*, Shore and Beach 59 (1), 17–26.

Appeaning Addo, K., Walkden, M., Mills, J.P., 2008. *Detection, measurement, and prediction of shoreline recession in Accra, Ghana*, ISPRS J. Photogramm. 63, 543–558. https://doi.org/10.1016/j.isprsjprs.2008.04.001

Basiński, T., Pruszak, Z., Tarnowska, M., Zeidler, R., 1993. *Sea coast protection*, IHE PAS, Gdańsk, 536 pp., (in Polish).

Boak, E.H. , Turner, I.L., 2005. *Shoreline definition and detection: A Review*, J. Coastal. Res. 21(4), 688–703. https://doi.org/10.2112/03-0071.1

Cohen, W.B, Kushla, J.D, Ripple, W.J, Garman, S.L., 1996. *An introduction to digital methods in remote sensing of forested ecosystems: Focus on the Pacific Northwest, USA*, Ecol. Envir. 20, 421–435. https://doi.org/10.1007/BF01203849

Collier P., Inkpen R., Fontana D., 2001. *The use of historical photography in environmental studies*, Cybergeo: Eur.

J. Geogr. 184.
https://doi.org/10.4000/cybergeo.4019

Constantino, D., Pepe, M., Dardanelli, G., Baiocchi, V., 2020. *Using optical satellite and aerial imagery for automatic coastline mapping*, Geographia Tech. 15(2), 171–190. https://doi.org/10.21163/GT_2020.152.17

Cooley, J.W., Tukey, J.W., 1965. *An algorithm for the machine calculation of complex Fourier series*, Math. Comput. 19, 297–301.

Cracknell, A., 1999. *Remote sensing techniques in estuaries and coastal zones – an update*, Int. J. Remote Sens. 19(3), 485–496.
https://doi.org/10.1080/014311699213280

Davis, J.D., Chojnacki, J.D., 2017. *Two-dimensional discrete Fourier transform analysis of karst and coral reef morphologies*, T GIS 21(13), 521–545.
https://doi.org/10.1111/tgis.12277

Dellepiane, S., Laurentiis, R., Giordano, F., 2004. *Coastline extraction from SAR images and a method for the evaluation of the coastline precision*, Pattern Recogn. Lett. 25(13), 1461–1470.
https://doi.org/10.1016/j.patrec.2004.05.022

Dolan, R., Hayden, B., Heywood, J., 1978. *A new photogrammetric method for determining shoreline erosion*, Coast. Eng. 2, 21–39.
https://doi.org/10.1016/0378-3839(78)90003-0

Dolan, R., Hayden, B., May, S., 1983. *Erosion of the US shorelines*, [in:] *Erosion of the US shorelines*, Komar, P.D. (Ed.), CRC Handbook of Coastal Processes and Erosion, CRC Press, Boca Raton FL, 285–299.

Dubrawski, R., 2000. *The impact of artificial beach replenishment of sea shores on the coastal zone of the Hel Peninsula in the period 1989–1997*, Sci. Publ. Dept. Maritime Institute, Gdańsk-Szczecin, 23–29, (in Polish).

Dudgeon, D.E., Mersereau, R.M., 1983. *Multidimensional Digital Signal Processing*, Prentice-Hall Signal Processing Ser., Prentice Hall, Englewood Cliffs, 406 pp.

Ferreira, O., Garcia,T., Matias, A., Taborda, R., Dias, J.A., 2006. *An integrated method for the determination of set-back lines for coastal erosion hazards on sandy shores*, Cont. Shelf. Res. 26, 1030–1044.
https://doi.org/10.1016/j.csr.2005.12.016

Furmańczyk, K., 1994. *Contemporary development of the coastal zone of the tidal sea in the light of remote sensing research on the Baltic coast*, Szczecin Univ. Press, Szczecin, 147 pp., (in Polish).

Furmańczyk, K., Musielak, S., 1993. *Analysis of changes and forecast of threats to the Hel Peninsula in the light of remote sensing research*, Inżynieria Morska i Geotechnika 1/1993, 351–362, (in Polish).

Gehrmann, A., Harding, Ch., 2018. *Geomorphological Mapping and Spatial Analyses of an Upper Weichselian Glacitectonic Complex Based on LiDAR Data, Jasmund Peninsula (NE Rügen), Germany*, Geosciences 8(208), 2–24.
https://doi.org/10.3390/geosciences8060208

Hughes, M.L., McDowell, P.F., Marcus, W.A., 2006. *Accuracy assessment of georectified aerial photographs: Implications for measuring lateral channel movement in a GIS*, Geomorphology 74, 1–16.
https://doi.org/10.1016/j.geomorph.2005.07.001

Idier, D., Falques. A., 2014. *How kilometric sandy shoreline undulations correlate with wave and morphology characteristics: Preliminary analysis on the Atlantic coast of Africa*, Advances in Geosciences 39, 55–60.
https://doi.org/10.5194/adgeo-39-55-2014

Jensen, J., 2000. *Remote sensing of the environment: An Earth resource perspective*, Prentice-Hall, 592 pp.

Kaczmarek, L., Ostrowski, R., Skaja, M., Szmytkiewicz, M., 1998. *Mathematical modeling of seashore changes at the base of the Hel Peninsula, taking into account artificial replenishment*, Inżynieria Morska i Geotechnika 1/1998, 13–25, (in Polish).

Khairulbahri, M., 2022. *The qualitative analysis of the nexus dynamics in the Pekalongan coastal area, Indonesia*, Sci. Rep. 12, 11391.
https://doi.org/10.1038/s41598-022-15683-9

Królikowski, L., Strzelecki, W., 1969. *Characteristics of the sands of coastal dunes*, Sylwian 12, 21–29, (in Polish).

Larson, M., Capobianco, M., Jansen, H., Rózyński, G., Southgate, H.N., Stive, M., Wijnberg, K.M., Hulscher, S., 2003. *Analysis and modeling of field data on coastal morphological evolution over yearly and decadal time scales. Part 1: background and linear techniques*, J. Coastal. Res. 19(4), 760–775.

List, J., Farris, A., 1999. *Large-scale shoreline response to storms and fair weather*, Proc. Coastal Sediments 99, Long Island, New York, 1324–1337.

Liu, H., Jezek, C., 2004. *Automated Extraction of Coastline from Satellite Imagery by Integrating Canny Edge Detection and Locally Adaptive Thresholding Methods*, Int. J. Remote Sens. 25, 937–958.
https://doi.org/10.1080/0143116031000139890

Moore, L.J., 2000. *Shoreline mapping techniques*, J. Coastal Res., 16(1), 111–124.

Morgan, E.L., Gergel, S., Coops, N., 2010. *Aerial photography: A rapidly evolving tool for ecological management*, Bioscience 60(1), 47–59.
https://doi.org/10.1525/bio.2010.60.1.9

Overton, M., Fisher, J., 1996. *Shoreline analysis using digital photogrammetry*, Proc. 25th Int. Conf. Coastal Eng. (Orlando, Florida), 3750–3761.

Paine, D., Kiser J., 2012. *Aerial Photography and Image Interpretation*, John Wiley & Sons, 648 pp.

Pelczar, M., Nejczew, P., Mielczarski, A., 1990. *Cartometric analysis of the shore-line changes on the eastern part of the Polish Baltic coast in the last century*, Rozprawy Hydrotechniczne, vol. 51, 69–113, (in Polish).

Prošek, A., Leskovar, M., 2015. *Use of fast Fourier transform for sensitivity analysis*, [in:] *Fourier Transform – Signal*

Processing and Physical Sciences, Salih, S.M. (Ed.), InTech Open, London, 227 pp. https://doi.org/10.5772/59769

Rayner, J.N., 1972. *The application of harmonic and spectral analysis to the study of terrain*, [in:] *Spatial Analysis in Geomorphology*, Chorley, R.J. (Ed.), Methuen, London, UK, 283–302.

Ricard, Y., Froidevaux, C., Simpson, R., 1987. *Spectral analysis of topography and gravity in the Basin and Range Province*, Tectonophysics 133, 175–187.

Shoshany, M., Degani, A., 1992. *Shoreline detection by digital image processing of aerial photography*, J. Coastal Res. 8(1), 29–34.

Stachurska, B., 2012. *Analysis of changes in the position of the Hel Peninsula coastline based on aerial photographs from 1947–1991*, Inżynieria Morska i Geotechnika 33 (4), 541–542, (in Polish).

Spagnolo, M., Bartholomaus, T.C., Clark, C.D., Stokes, C.R., Atkinson, N., Dowdeswell, J.A., Ely, J.C., Graham, A.G.C., Hogan, K.A., King, E.C., Larter R.D., Livingstone S.J., Pritchard H.D., 2017. *The periodic topography of ice stream beds: Insights from the Fourier spectra of megascale glacial lineations*, J. Geophys. Res.-Earth 122, 1355–1373. https://doi.org/10.1002/2016JF004154

Tomczak, A., 1995. *Geological structure and evolution of the Polish coastal zone*, J. Coastal Res. 22, 15–31.

Tuominen, S., Pekkarinen, A., 2004. *Local radiometric correction of digital aerial photographs for multisource forest inventory*, Remote Sens. Environ. 89, 72–82. https://doi.org/10.1016/j.rse.2003.10.005

Urbański, J., 2001. *Cartographic modeling of the coastal zone of the sea*, Gdańsk University Press, Gdańsk, (in Polish).

Uścinowicz, Sz., Kramarska, R., Kaulbarsz, D., Jurys, L., Frydel, J., Przezdziecki, P., Jedliński, W., 2014. *Baltic Sea coastal erosion; a case study from the Jastrzębia Góra region*, Geologos 20(4), 259–268. https://doi.org/10.2478/logos-2014-0018

Yang, J., Seo, D., Lim, H., Choi, Ch., 2010. *An analysis of coastal topography and land cover changes at Haeundae Beach, South Korea*, Acta Astronaut. 67, 1280–1288. https://doi.org/10.1016/j.actaastro.2010.06.013

Zawadzka-Kahlau, E., 1999. *Development tendencies of the Polish shores of the South Baltic Sea*, Gdańsk Science Association, Gdańsk, 147 pp., (in Polish).